

비에혼합 튜브형상내 화염셀의 거동에 대한 수치 해석적 연구

박현수* · 유춘상**

A Numerical Study of the Flame Cell Dynamics in Opposed Nonpremixed Tubular Configuration

Hyunsu Park*, Chun Sang Yoo**

ABSTRACT

The flame cell dynamics in 2-D opposed nonpremixed tubular configuration was investigated using high-fidelity numerical simulations. The diffusive-thermal instability occurs as the Damköhler number, Da , approaches the 1-D extinction limit of the tubular flames and several flame cells are generated depending on Da , and flame radius. In general, the number of flame cells are found close to the largest wave number from the linear stability analysis. It was also found from the displacement speed analysis that during the local flame extinction and cell formation, negative edge flame speed is observed due to small gain from reaction compared to large loss from diffusion.

Key Words : Diffusive-thermal instability, Opposed nonpremixed tubular flame, Linear stability analysis, Damköhler number, Flame cell.

The characteristics of opposed premixed and nonpremixed tubular flames have been widely investigated by experiments and numerical simulation [1-4]. It is already known that the diffusive-thermal instability near flame extinction limit appears when the Lewis number is less than unity. In the opposed nonpremixed tubular configuration, flame cells can also be observed near the extinction limit. The each end of a flame cell is the flame edge, and the temperature at edge of the flame cell is locally high by mass concentration of fuel.

In this study, the flame cell dynamics in opposed nonpremixed tubular configuration were investigated by using the conventional linear stability analysis and various case studies with high-fidelity numerical simulations. By assuming 1-step overall reaction, constant density, no azimuthal direction velocity the nondimensional 1-D governing equations (Eq. (1)), boundary conditions (Eqs. (2)), and the radial velocity which is function of r , (Eqs. (3)) can be

modeled as follows.

$$\tilde{u}_r \frac{d}{d\tilde{r}} \begin{pmatrix} \tilde{T} \\ \tilde{Y}_F \\ \tilde{Y}_O \end{pmatrix} = \frac{1}{\tilde{r}} \frac{d}{d\tilde{r}} \left(\tilde{r} \frac{d}{d\tilde{r}} \right) \begin{pmatrix} \tilde{T} \\ \tilde{Y}_F/L_F \\ \tilde{Y}_O/L_O \end{pmatrix} \quad (1)$$

$$+ Da \tilde{Y}_F \tilde{Y}_O e^{-\tilde{T}_a/\tilde{T}} \begin{pmatrix} q \\ -\alpha_F Y_{O2} \\ -\alpha_O Y_{F1} \end{pmatrix}$$

$$\begin{aligned} \tilde{T} &= \tilde{T}_2, \tilde{Y}_F = 0, \tilde{Y}_O = 1, \tilde{u}_r = -1, \text{ at } \tilde{r} = \tilde{r}_2, \\ \tilde{T} &= \tilde{T}_1, \tilde{Y}_F = 1, \tilde{Y}_O = 0, \tilde{u}_r = \tilde{u}_{r,1}, \text{ at } \tilde{r} = \tilde{r}_1, \end{aligned} \quad (2)$$

$$u_r(r) = \begin{cases} u_{r,1} \frac{r_1}{r} \sin \left(\frac{u_{r,2}}{u_{r,1}} \frac{r_2}{r_1} \sqrt{\frac{Q}{4}} \left(\frac{r}{r_2} \right)^2 + \frac{\Pi}{2} - \frac{u_{r,2}}{u_{r,1}} \frac{r_1}{r_2} \sqrt{\frac{Q}{4}} \right) \\ u_{r,2} \frac{r_2}{r} \sin \left(\sqrt{\frac{Q}{4}} \left(\frac{r}{r_2} \right)^2 + \frac{\Pi}{2} - \sqrt{\frac{Q}{4}} \right) \end{cases} \quad (3)$$

Y_F is the fuel mass fraction, Y_O is the oxidizer mass fraction, Da is the Damköhler number, q is the heat release rate, T_a is the activation energy, L_F is the Lewis number of the fuel, L_O is the Lewis number of the oxidizer, and Q is the pressure eigenvalue. The fuel issue from inner nozzle, r_1 , and the oxidizer issue from outer nozzle, r_2 .

* 울산과학기술대학교 기계 및 원자력공학부

† 연락저자, csyoo@unist.ac.kr

TEL : (052)217-2322 FAX : (052)-217-2409

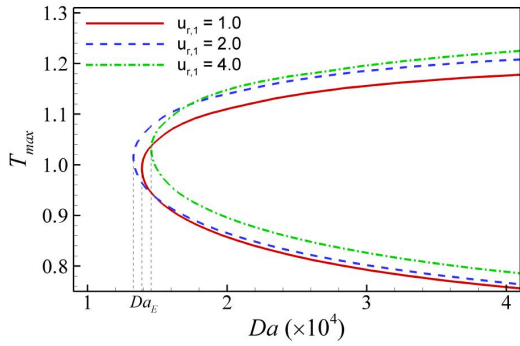


Fig. 1 Maximum flame temperature as a function of the Damköhler number as $u_{r,1}=1, 2,$ and 4.

The parameters for Eq. (1) are specified as follows: $q=1.2$, $\tilde{T}_a=8$, $L_F=0.3$, $L_O=1.0$, $\alpha_F Y_{O_2}=1.0$, $\alpha_O Y_{F,1}=0.36$, $\tilde{r}_1=20$, $\tilde{r}_2=100$, $\tilde{T}_1=\tilde{T}_2=0.2$, and $\tilde{u}_{r,1}$. The fuel Lewis number is specified as 0.3 to investigate the diffusive-thermal instability near extinction limit.

The Eqs. (1) with different fuel velocity, $u_{r,1}=1, 2,$ and 4, were solved by using a finite difference and a simple continuation method. Figure 1 shows the so-called “C-curve” exhibiting the extinction limits according to the different fuel speeds. The extinction Damköhler number, Da_E is approximately 13,894, 13,287, and 14,568 as $\tilde{u}_{r,1}$ is increased.

The conventional linear stability analysis [5] was conducted for the 1-D governing equations, which leads to an eigenvalue problem, $\mathbf{A}\mathbf{x} = \lambda\mathbf{B}\mathbf{x}$. The detailed procedure can be found in [5]. The relationship between λ the amplification factor in time, and k the wavenumber in the azimuthal direction can be drawn for different Da .

Figure 2 shows that the maximum $\text{Re}(\lambda)$ as a function of k for different Da and $u_{r,1}$. Positive $\text{Re}(\lambda)$ implies that any small fluctuations in the solution can lead to the instability of the solution. Therefore, the flames may become unstable and cellular instability may occur in opposed nonpremixed tubular flames.

The largest $\text{Re}(\lambda)$ occurs at different wave number for different Da (see Table 1). For cases with $u_{r,1} = 1, 2,$ and 4, the largest $\text{Re}(\lambda)$ occurs approximately at $k = 7, 10,$ and 14,

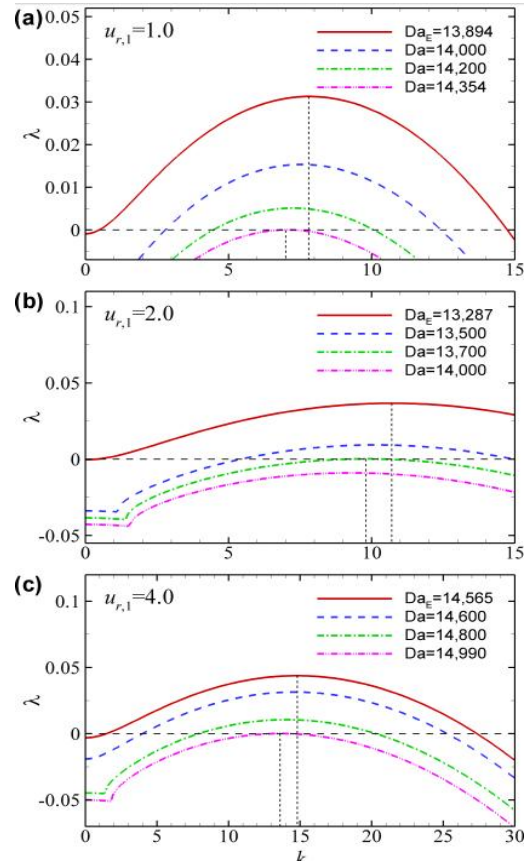


Fig. 2 Largest $\text{Re}(\lambda)$ as a function of wave-number, k , for different Da and $u_{r,1}=1, 2,$ and 4.

which are similar to the number of flame cells observed in 2-D simulations. This issue will be discussed later. For cases with $u_{r,1} = 1, 2,$ and 4, positive $\text{Re}(\lambda)$ appears at Da greater than Da_E and its range varies with different $u_{r,1}$. For details, see Table 1.

Table 1 k at which the largest $\text{Re}(\lambda)$ occurs and Da range for $u_{r,1}=1, 2,$ and 4.

$u_{r,1}$	k	Da range for $\text{Re}(\lambda) > 0$
1	$7 \leq k \leq 7.8$	$Da_E \leq Da \leq 14,354$
2	$9.8 \leq k \leq 10.7$	$Da_E \leq Da \leq 13,700$
4	$13.6 \leq k \leq 14.8$	$Da_E \leq Da \leq 14,990$

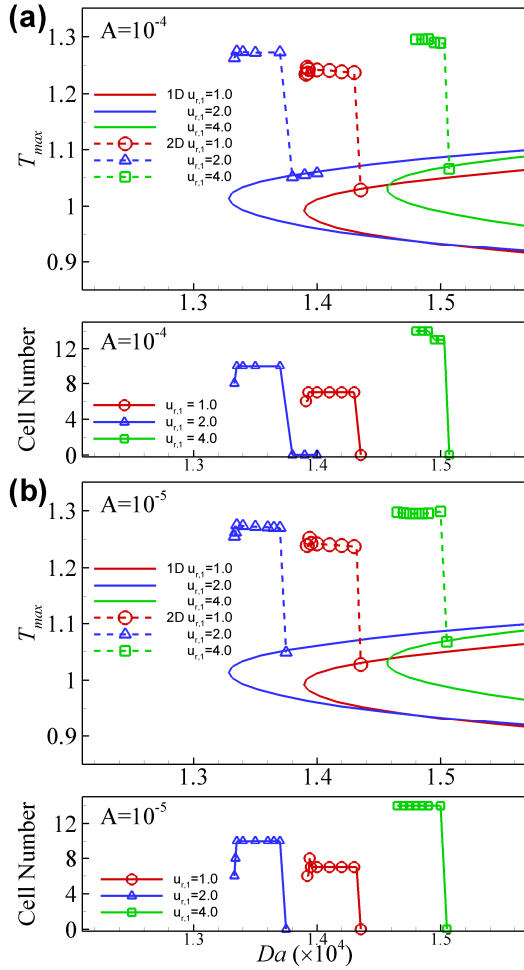


Fig. 3 Maximum temperature vs. Da for 1-D and 2-D solutions, and cell number vs. Da for 2-D cases as $u_{r,1}=1, 2,$ and 4 with (a) $A=10^{-4}$ and (b) $A=10^{-5}$.

2-D numerical simulations were performed based on the above linear stability analysis and 1-D solutions at each Da . An 8th-order central difference scheme for spatial derivatives and a 4th-order Runge-Kutta method for time integration method are used with the message passing interface (MPI) for parallel computing [6]. We used two different 2-D initial temperature conditions. First, small fluctuation is added to 1-D temperature solution as in Eqs. (4). The constant A is the perturbation amplitude and chosen as 10^{-4} and 10^{-5} in this study. Second, ‘C’ formed temperature profile is used Eqs. (5). The parameters are $y1=0.5\pi,$ $y2=1.5\pi,$ and $\sigma=0.1\pi$.

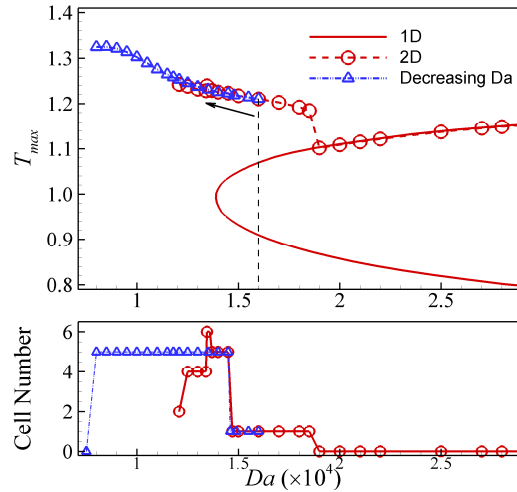


Fig. 4 Maximum temperature vs. Da for 1-D and 2-D solutions, maximum temperature at Da decreasing from $Da=16,000,$ and cell number vs. Da for 2-D cases as $u_{r,1}=1$ with C-initial condition.

$$\tilde{T}_{2D,init}(r, \theta) = \tilde{T}_1 + (1 + A \sin\theta)(\tilde{T}(r) - \tilde{T}_1) \quad (4)$$

$$\tilde{T}_{2D,init}(r, \theta) = \tilde{T}_1 + 0.5(\tilde{T}(r) - \tilde{T}_1) \times (\tanh((\theta - y_1)/\sigma) - \tanh((\theta - y_2)/\sigma)) \quad (5)$$

Figure 3 shows the maximum temperature and number of cells for different A values. For cases with $u_{r,1} = 1$ with $A=10^{-4}$, the cellular instability occurs approximately in the range of $Da \approx 14,350$ to $Da \approx 13,907$. The number of cells changes from 7 to 6. For cases with $u_{r,1}=2$, the cellular instability occurred from $Da \approx 13,700$ to $Da \approx 13,320$, and the cell number changes from 10 to 8. For cases with $u_{r,1}=4$, the cellular instability is observed from $Da \approx 15030$ to $Da \approx 14650$. The change of cell number was 13 to 14. For cases with A of 10^{-5} , the same 2-D simulations were conducted again. For cases with $u_{r,1} = 1$, the cellular instability occurs approximately at $Da \approx 14,330$ down to $Da \approx 13,915$. The number of cells changes from 7, 8-6. For cases with $u_{r,1} = 2$, the cellular instability occurs from $Da \approx 13,700$ to $Da \approx 13,325$, and the order of cell number change was 10-8-6. For cases with $u_{r,1} = 4$, cellular instability was observed from $Da \approx 15030$ to $Da \approx 14650$. The number of cells is 14.

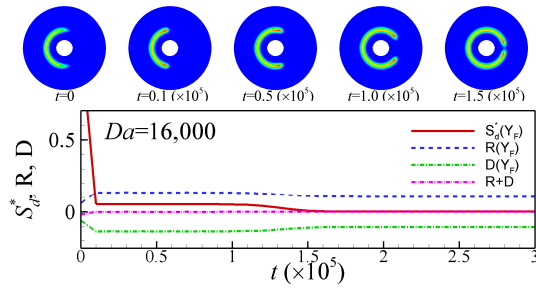


Fig. 5 The temperature, S_d , R , D and $R + D$ vs. time for case with $Da = 16,000$, $u_{r,1} = 1$, C-shaped initial condition.

For two different A cases, the number of cells in mostly unstable region was equal to results of k (7, 10, and 14) except the extinction limit. This result implies that the unstable Da region and cell number for each case can be expected through the results of the linear stability analysis. Further simulations with smaller A of 10^{-6} show that there is no change of number of cells even though the transition from the initial condition to the steady-state is little bit different. Therefore, it can be deduced from the results that different levels of perturbation can lead to different results in the cellular instability. The maximum temperature is proportional to cell number, which has inversely proportional cell length, because the temperature is increased by the focusing effect of fuel of which Lewis number is less than unity.

Figure 4 shows the results using C-shaped initial condition of Eq. (5). The 2-D extinction limit extended down to $Da = 12,082$ and the order of changed cell number is 1-5-6-4-2 from the onset of unstable flame, which is quite different from the previous results and linear stability analysis. This implies that opposed nonpremixed tubular flame is quite sensitive to initial condition. The tubular flame instability was investigated with decreasing Da from $Da = 16,000$ similar previous experiments [1-2]. It is different from previous studies, because Da is changed to little small Da with maintaining a state of previous Da . The cell number was changed from 1 to 5 at the same Da at which 5 flame cells first appeared in just 2-D study. Then, the cell number, 5, was remained and maximum temperature

continuously was increased. Finally, the extinction limit was extremely extended to $Da \approx 7,500$.

Figure 5 shows propagation speed of edge flame, S_d , reaction rate of Y_F , $S_{d,R}$ diffusion rate of Y_F , $S_{d,D}$, and $S_{d,R} + S_{d,D}$ for the case with $Da = 16,000$, $u_{r,1} = 1$ and C-shaped initial condition. The displacement speed is defined by:

$$S_d = S_{d,R} + S_{d,D} = \frac{1}{\rho |\nabla Y_F|} (\dot{\omega}_F + \nabla^2 (Y_F / Le_F)) \quad (6)$$

At first, large S_d rapidly drop to 0.052. This value maintained at $t = 0.9 \times 10^5$, and it vanishes. There is no more movement of the tubular flame from $t = 1.5 \times 10^5$. $S_{d,R} + S_{d,D}$ vanishes when the flame do not move any more.

The flame cell dynamics in various conditions were investigated using the linear stability analysis and 2-D high-fidelity simulations. The maximum temperature, cell number, and S_d were analyzed to figure out the diffusive-thermal instability of tubular flames.

Acknowledgments

This study was supported by Basic Science Research Program through the National Research Foundation of Korea (NRF) funded by the Ministry of Education, Science and Technology (No. 2011-0008201). HP was also supported by BK21Plus funded by the Ministry of Education.

References

- [1] S. Hu, P. Wang, R. W. Pitz, *Proc. Combust. Inst.*, 31, 2007, 1093-1099.
- [2] S. Hu, R. W. Pitz, *Combust. Flame* 156, 2009, 51-61.
- [3] S. Hu, R. W. Pitz, Y. Wang, *Combust. Flame* 156, 2009, 90-98.
- [4] S. W. Shopoff, P. Wang, R. W. Pitz, *Combust. Flame* 158, 2011, 876-884, 2165-2177.
- [5] M. Short, J. Buckmaster, S. Kochevets, *Combust. Flame* 125, 2001, 893-905.
- [6] C. S. Yoo, J. H. Frank, J. H. Chen, *Combust. Flame* 156, 2009, 140-151.
- [7] H. G. Im and J. H. Chen, *Combust. Flame* 119, 1999, 436-454